FOSSIL TURBULENCE

C. H. Gibson, University of California, San Diego, La Jolla, CA, USA

doi:10.1006/rwos.2001.0138

Introduction

Fossil turbulence processes are central to turbulence, turbulent mixing, and turbulent diffusion in the ocean and atmosphere, in astrophysics and cosmology, and in other natural flows. However, because turbulence is often imprecisely defined, the distinct and crucial role of fossil turbulence may be overlooked. Turbulence occurs when inertial-vortex forces $\vec{v}\times\vec{\omega}$ dominate all other forces for a range of length and timescales to produce rotational, eddy-like motions, where $\vec{v}$ is the velocity and $\vec{\omega}$ is the vorticity $\nabla\times\vec{v}$. Turbulence originates at length scales with the smallest overturn times; that is, at the viscous Kolmogorov length scale $L_K \equiv (\nu^3/\varepsilon)^{1/4}$ and timescale $T_K \equiv (\nu/\varepsilon)^{1/2}$, where ν is the kinematic viscosity of the fluid and ε is the viscous dissipation rate. In stratified fluids with gravity, turbulence appears in bursts on tilted density layers to produce patches (see **Figure 3**). Turbulence then cascades, driven by $\vec{v}\times\vec{\omega}$ forces, to larger scales where buoyancy forces cause fossilization of vertical motions at the Ozmidov scale $L_R \equiv (\varepsilon/N^3)^{1/2}$, where N is the ambient stratification frequency. Coriolis forces may also cause fossilization, usually of horizontal motions, at the Hopfinger scale $L_H = (\varepsilon/\Omega^3)^{1/2}$, where Ω is the angular velocity. In the ocean and atmosphere this may occur at large horizontal scales when Ω is the vertical component of the planetary angular velocity, or at any scale where L_H is smaller than the eddy size; for example, in the spin up of Kelvin–Helmholtz billows. Turbulence is defined as an eddy-like state of fluid motion where the inertial vortex forces of the eddies are larger than any other forces that tend to damp the eddies out. Fossil turbulence is defined as any fluctuation in a hydrophysical field such as temperature, salinity, or vorticity that was produced by turbulence and persists after the fluid is no longer turbulent at the scale of the fluctuation. Fossil turbulence patches persist much longer than the turbulence events that produced them because they must mix away, but with smaller dissipation rates, the same velocity and scalar variances that existed in their original turbulence patches. Fossil turbulence preserves information about the original turbulence and completes the mixing and diffusion processes initiated by stratified turbulence bursts.

The first printed reference to the concept of fossil turbulence was apparently when George Gamov suggested in 1954 that galaxies might be fossils of primordial turbulence produced by the Big Bang. Although it now appears that the primordial fluid at the time of galaxy formation was too viscous and stratified to be strongly turbulent, the Gamov concept that information about irreversible hydrodynamic states and processes might be preserved by parameters of the structures formed was quite correct and is concisely captured by the term 'fossil turbulence'. Persistent refractive index patches caused by mountain wakes in the stratified atmosphere and detected by radar were recognized as fossils of turbulence, causing organizers and participants to form a Fossil Turbulence working group for the 1969 Stockholm Colloquium on Spectra of Meteorological Variables. Woods showed that billows made visible by introducing dye in the interior of the stratified ocean formed highly persistent remnants of these turbulent events, as demonstrated by Thorpe in the laboratory using a tilt tube. The first use of the expression 'fossil turbulence' was attributed to Woods. Patches of strong oceanic temperature microstructure measured without velocity microstructure from a submarine were termed 'footprints of turbulence' by Stewart. However, two important assumptions were that no universal fossil turbulence description is possible and that all vertical velocity fluctuations vanish in fossil turbulence. Both are incorrect. A universal similarity theory of stratified fossil turbulence was presented by Gibson in 1980. Universal constants and spectral forms of stratified fossil turbulence were estimated by the theory (see **Figure 1**), and hydrodynamic phase diagrams were introduced as a method for classifying temperature and salinity microstructure patches in the ocean interior according to their hydrodynamic states (turbulent, active-fossil turbulence, completely fossil) and for extracting fossilized information about the previous turbulence and mixing. Furthermore, it was shown that turbulent kinetic energy is trapped and preserved in fossil turbulence as saturated internal wave motions termed fossil-vorticity-turbulence. The 1980 theory has been confirmed and extended to describe fossilized turbulence produced by magnetic forces, self-gravitational forces, and space-time inflation in a new theory of gravitational structure formation.

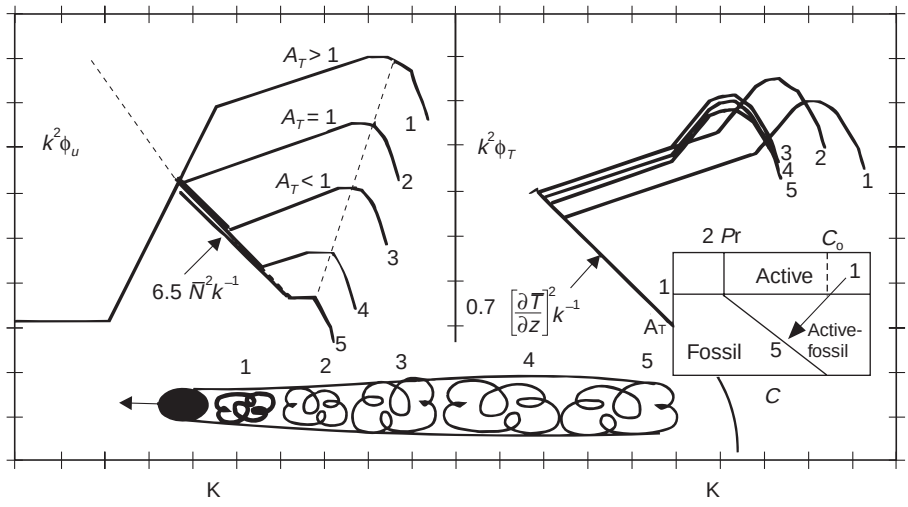

Figure 1 Dissipation spectra $k^2\phi_u$ for velocity (left) and temperature $k^2\phi_T$ (right) for active turbulence in water as it fossilizes, represented by five stages of the temperature stratified turbulent wake shown at the bottom or, equivalently, at increasing times after the onset of turbulence in a patch. (Reproduced from Gibson, 1999.) Universal spectral forms for the saturated internal waves of the remnant fossil-vorticity-turbulence and fossil-temperature- turbulence microstructure patch are from Gibson (1980). The trajectory on an $A_T \equiv (\varepsilon/\varepsilon_o)^{1/2}$ versus Cox number C hydrodynamic phase diagram is shown in the right insert. Temperature dissipation rates χ provide a conservative estimate of ε_o from the expression $\varepsilon_o \geq 13DCN^2$.

Fossil turbulence patches have been misinterpreted as turbulence patches in oceanic turbulence sampling experiments that fail to account for the turbulent fossilization process. Such mistakes have led to large underestimates of the true average vertical turbulence flux rates in many ocean layers, and are the source of the so-called by Tom Dillon 'dark mixing' paradox of the deep ocean interior. Dark mixing is to the ocean as dark matter is to galaxies. Dark matter is unseen matter that must exist to prevent galaxies from flying apart by centrifugal forces. Dark mixing is mixing by turbulence events that must exist to explain why some layers in the ocean interior are well mixed, but have strong turbulent patches that are undetected except for their fossil turbulence remnants. Both the dark mixing and dark matter paradoxes appear to be manifestations of the same problems; that is, extreme intermittency of nonlinear cascade processes over a wide range of values leading to extreme undersampling errors, and basic misunderstandings about the underlying irreversible fluid mechanics. Observations of fossil turbulence patches of rare, powerful, but undetected turbulence events in the deep ocean support the statistical evidence (**Figure 2**) that bulk flow estimates of the vertical diffusivity in the deep main thermocline are correct, rather than interpretations of sparse temperature dissipation rate χ measurements that claim large discrepancies but do not take into account either the extreme intermittency of χ in deep ocean layers or the fossil turbulence evidence.

Fossil turbulence signatures in hydrophysical fields preserve information about previous turbulence. Temperature fluctuations produced by turbulence are termed fossil-temperature-turbulence for fluctuations at length scales where the turbulence has been damped by buoyancy. Skywriting rapidly becomes fossil-smoke-turbulence above the inversion layer. The larger the vertical fossil temperature turbulence patch size L_P, the larger the viscous and temperature dissipation rates ε and χ must have

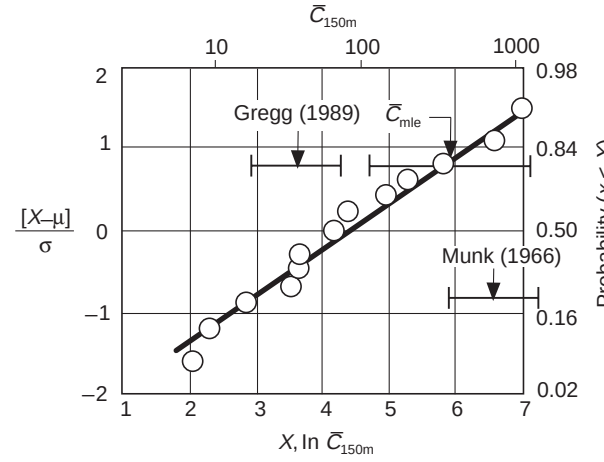

Figure 2 Normalized lognormal probability plot of dropsonde Cox number samples, averaged over 150 m in the vertical, in the depth range 75–1196 m. Estimated 95% confidence intervals are shown by horizontal bars, and compared to confidence intervals for C from the Gregg (1989) and Munk (1966) models for the thermocline, by Gibson (1991).

been in the original patch of turbulence. Fossil turbulence remnants are the footprints and scars of previous turbulent events, and redundantly preserve information about their origins in a wide variety of oceanic fields such as temperature, salinity, bubbles, and vorticity. The process of extracting information about previous turbulence and mixing from fossil turbulence is termed hydropaleontology.

Stratified and rotating fossils of turbulence are more persistent than their progenitor turbulence events because they possess almost the same velocity variance (kinetic energy) and scalar variance (potential entropy of mixing) as the original turbulent field, but have smaller viscous and scalar dissipation rates of these quantities than they had while they were fully turbulent just prior to the beginning of fossilization. The most powerful turbulence events produce the most persistent fossils, with persistence times proportional to the normalized Reynolds number $\varepsilon_0/\varepsilon_F$ and inversely proportional to the ambient stratification frequency N, where $\varepsilon_0 \approx 0.4L_T^2N^3$ is the estimated dissipation rate at beginning fossilization and $\varepsilon_F = 30\nu N^2$ is at complete fossilization, where $L_T \approx L_P$ is the maximum Thorpe overturning scale of the patch. Oceanic fossil turbulence processes are more complex and important than in nonstratified nonrotating flows where the only mechanism of fossilization is the viscous damping of turbulence before mixing is complete and all scalar fields become singly connected. Laboratory viscous fossil turbulence without stratification or rotation is thus mentioned in textbooks only as a curiosity of flow visualization, where eddy patterns of dye or smoke that appear to be turbulent are not because the turbulent fluid motions have been damped by viscosity. Buoyancy-fossils and rotation-fossils are difficult to study in the laboratory or in computer simulation because of the wide range of relevant length and timescales.

Most of the ocean's kinetic energy exists as fossil-vorticity-turbulence because its motions, driven by thermohaline oceanic circulation, air–sea interaction of atmospheric motions and tidal forces of the sun and moon, are converted into turbulence energy at the top and bottom ocean surfaces by turbulence formation and its cascade to larger scales, and are not immediately or locally dissipated. Instead, oceanic turbulent kinetic energy and its induced scalar-potential-entropy is fossilized by buoyancy and Coriolis forces and distributed oceanwide by advection, leaving fossil-scalar-turbulence and fossil-vorticity-turbulence remnants in a variety of hydrodynamic states. These turbulence fossils move and interact with their environment and each other in the ocean interior by mechanisms that are poorly understood and hardly recognized. For example, a necessary stage of average double-diffusive vertical fluxes in the ocean may be fluxes driven by double-diffusive convection in the final stages of fossil-temperature-salinity-turbulence decay within fossil-temperature-salinity-turbulence patches. The turbulence event scrambles the pre-existing temperature and salinity fields to produce a stirred field in which the full range of possible double-diffusive instabilities occur. These drive motions in the late stages of the turbulent fossil decay, leaving characteristic layered structures of salt fingering. Convective instabilities at low Rayleigh number, insufficient to drive turbulent motion, may also occur.

Powerful turbulence events produce fossils that radiate wave energy and trigger secondary turbulence events at their boundaries; this turbulence also fossilizes, and these fossils produce more turbulence (**Figure 3**). Turbulent mixing and diffusion is initiated by turbulence, but the final stages of the mixing and diffusion are completed only after the flow has become partially or completely fossilized. In practice, complete fossilization rarely occurs in the ocean because propagating internal waves produce strong shears at the strong density gradients of fossil density turbulence boundaries through baroclinic torques $\nabla\rho \times \nabla p/\rho^2$, where ρ is density and p is pressure. Active turbulence that arises in this way from patches of fossil turbulence is known as zombie turbulence.

History of Fossil Turbulence

The distinctive, eddy-like-patterns of turbulent motions are beautiful and easily recognized. Many ancient civilizations have woven them into their arts, religions, and sciences. The first attempts at hydropaleontology were applications of Kolmogorovian universal similarity theories of turbulence to cosmology by members of the Soviet school of turbulence. Recent evidence from space telescopes suggests that primordial turbulence and density structure from the Big Bang were fossilized at 10^{-35} s by inflation of space beyond the length scales of causal connection ct of the fluctuations, where c is the speed of light and t is the time. This fossilized microstructure seeded the formation of all subsequent structures in a zombie-turbulence fossil-turbulence cascade, similar to that in the ocean, that preserves evidence of the hydrophysical states of each stage of the process in various hydrodynamic fossils.

The 1969 working group on fossil turbulence examined patches of persistent refractive index fluctuations produced by turbulence in the stratified

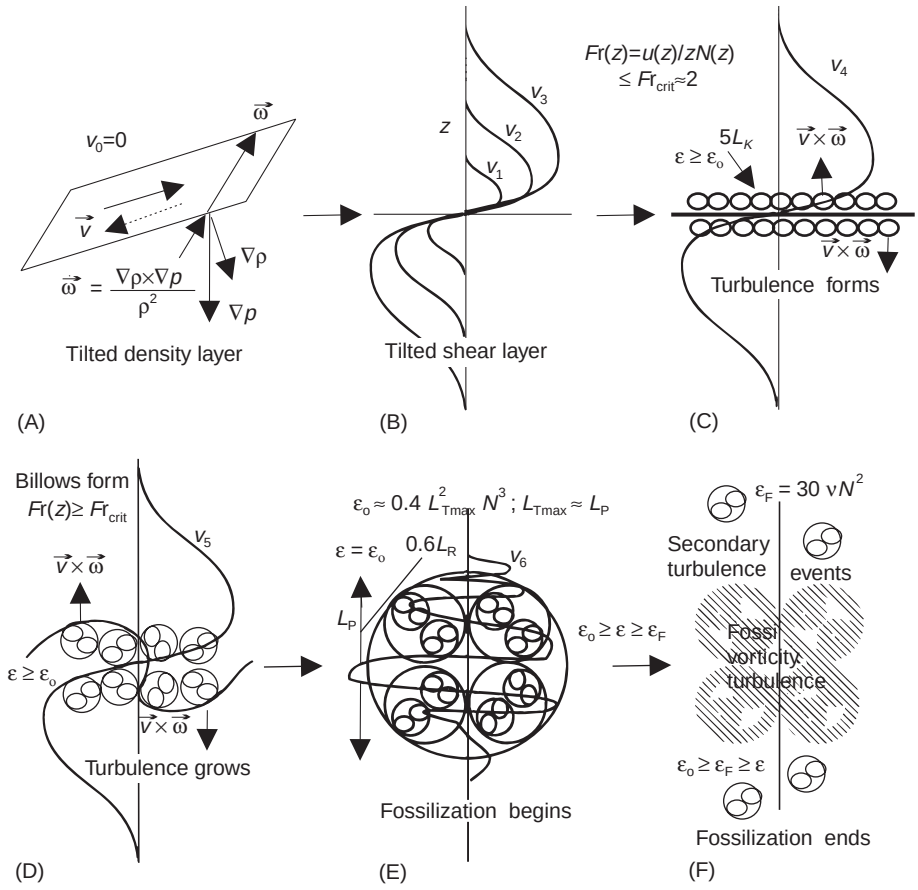

Figure 3 Fossil turbulence formation on a suddenly tilted density layer in a stagnant stratified fluid. Baroclinic torques cause a buildup of vorticity on the density surface (A) with laminar boundary layers v_1 to v_3 (B). These become turbulent at 5–10 times the Kolmogorov scale L_K, steepening the density gradient and permitting storage of potential turbulent kinetic energy (C). Turbulent billows form and absorb the stored kinetic energy. The strong density interface is broken to form the first billow at a critical turbulent boundary layer scale when $Fr(z) \geq Fr_{crit} \approx 2$ (D). Turbulence cascades to larger vertical scales limited by 0.6 times the Ozmidov scale L_R where fossilization begins (E). leaving a fossil-vorticity-turbulence remnant. This decays by viscous dissipation and vertical radiation of internal waves that may form secondary turbulence events (F). Microstructure patches are actively turbulent if $\varepsilon \geq \varepsilon_o$, partially fossilized for $\varepsilon_o \geq \varepsilon \geq \varepsilon_F$, and fossil for $\varepsilon_F \geq \varepsilon$.

atmosphere and fluctuating temperature and dye patches produced by turbulence in the ocean interior which could not possibly be turbulent at the time of their detection. Scuba divers observed dye patch fossils of breaking internal waves from their turbulent beginning until they became motionless. Temperature microstructure patches were reported from a submarine with and without measurable velocity fluctuations, indicating that those without must be fossilized. Fossil turbulence patches produced in the stratified atmosphere by wind over mountains and wakes of other aircraft are dangerous to aircraft because of their long persistence times and powerful fossil-vorticity-turbulence. For example, a fossil turbulence patch sent passengers flying into the ceiling of a Boeing 737 at 24 000 feet on the afternoon of 3 September 1999, bound from Los Angeles to San Francisco, injuring 15 of the 107 passengers and five crew aboard. Detectable refractive index fluctuations from billow turbulence events behind mountains are observed many kilometers downstream by radar scattering measurements, long after all turbulence and fossil-vorticity-turbulence have been damped by buoyancy forces as shown by the layered anisotropy that develops in the radar returns. Fossils of clear air turbulence (CAT) (referred to as 'angels') have long been well known to radar operators. Equivalent dominant turbulent patches of the deep ocean have not yet been detected in their actively turbulent states.

The quantitative universal similarity theory of stratified fossil turbulence published in 1980 was based on towed-body small-scale temperature measurements made by Schedvi in 1974 in the upper ocean of the Flinders Current off Australia in a US–Soviet intercomparison cruise on the *Dmitri*

Mendeleev. The data showed clear evidence of buoyancy effects causing departures from spectral forms of the Kolmogorov and Batchelor universal similarity theories of turbulence and turbulent mixing. These departures were attributed to stratified turbulence fossilization. Key ideas of the theory are illustrated in **Figure 1** by the time evolution of velocity spectra ϕ_u and temperature spectra ϕ_T at five stages in a turbulent wake as the turbulence is fossilized by buoyancy forces. The integral of ϕ_u over wavenumber k is the velocity variance and the integral of ϕ_T is the temperature variance, where the Prandtl number ν/D is about 10 (corresponding to that of sea water) with D the thermal diffusivity. Spectra are multiplied by k^2 so their integrals represent velocity and temperature gradient variances, respectively proportional to the dissipation rates ε and χ.

Stage 1 of the turbulence patch is fully turbulent with turbulent activity coefficient $A_T > 1$ ($\varepsilon > \varepsilon_o$, where ε_o is the value at beginning of fossilization). Velocity dissipation spectra $k^2\phi_u$ for stages 1–5 along the wake are shown on the left of **Figure 1**. Each has integral $\varepsilon/3\nu$. Inertial subranges with slope $+1/3$ reflect Kolmogorov's second hypothesis for wavenumbers $k \approx 2\pi/L$ between the energy (or Obukhov) scale L_O (small k) and the Kolmogorov scale L_K (large k). The turbulence continues its cascade to larger L_O scales by entrainment of external nonturbulent fluid until the increasing L_O is matched by the decreasing Ozmidov scale $L_R = (\varepsilon/N^3)^{1/2}$ at the beginning of fossilization, where $\varepsilon = \varepsilon_o$, with spectral forms 2. The temperature dissipation spectrum $k^2\phi_T$ increases in amplitude from stage 1 to stage 2 as vertical temperature differences are entrained over larger vertical scales (even though the velocity spectrum $k^2\phi_u$ decreases) with increasing area $\chi/6D = C(\partial\overline{T}/\partial z)^2/3$, where χ is the diffusive dissipation rate of temperature variance and Cox number C is the mean square over square mean temperature gradient ratio. The dramatic differences in spectral shapes between the velocity dissipation spectra and the temperature dissipation spectra in **Figure 1** reflect the theoretical result that without radiation, the kinetic energy of powerful fossilized turbulence events persist as fossil-vorticity-turbulence for longer periods than the temperature variance persists as fossil-temperature-turbulence. This is the basis of the $A_T \equiv (\varepsilon/\varepsilon_o)^{1/2}$ versus C hydrodynamic phase diagram shown at the bottom right of **Figure 1**. Because χ and C are large in the temperature fossil, the velocity dissipation rate ε at the beginning of fossilization ε_o can be estimated from C using $\varepsilon_o \approx 0.4L^2{}_T N^3 \geq 13DCN^2$. The turbulent activity coefficient $A_T \equiv (\varepsilon/\varepsilon_o)^{1/2}$ is greater than 1 for stratified turbulence patches before fossilization, and less than 1 after fossilization begins. A particular patch decays along a straight line trajectory in the hydrodynamic phase diagram until $\varepsilon = \varepsilon_F \equiv 30\nu N^2$ at complete fossilization. It can be shown that C averaged over a large horizontal layer in the stratified ocean for a long time period is a good measure of the turbulent heat flux divided by the molecular heat flux, with the vertical turbulent diffusivity $K = DC$. The motivation for most oceanic microstructure measurements is to estimate K through measurements of the average C for various oceanic layers. The problem is that C, ε, and χ in the ocean, atmosphere, and in all other such natural flows with wide spacetime cascade ranges, tend to be extremely intermittent.

Intermittency of Oceanic Turbulence and Mixing

Turbulence with the enormous range of length scales possible in oceanic layers is very intermittent in space and time. Sampling turbulence and turbulent mixing without recognizing this intermittency and without recognizing that most oceanic microstructure is fossilized or partially fossilized has led to misinterpretations and errors in estimates of turbulent diffusion and mixing rates, especially in the deep ocean interior and in strong equatorial thermocline layers where intermittencies of ε and χ are maximum. Dissipation rates ε and χ are random variables produced by nonlinear cascades over a wide range of scales, resulting in lognormal probability density distributions and mean values larger than the mode values by factors in the range 10^2–10^5. Since the mode of a distribution is the most probable measured value, sparse microstructure studies will significantly underestimate mean ε and χ values, as well as any vertical exchange coefficients and flux estimates of heat, mass, and momentum that are derived from these quantities. For lognormal random variables, $G_X = \exp[3\sigma^2_{\ln X}/2]$, where the variance $\sigma^2_{\ln X}$ is the intermittency factor of a lognormal random variable X. Intermittency factors $\sigma^2_{\ln\chi}$ and $\sigma^2_{\ln\varepsilon}$ in the ocean have been measured, and range from typical values of 5 at midlatitudes near the surface, to 6 or 7 in the deep ocean and at equatorial latitudes. Thus, probable undersampling errors for these quantities range from $G_{\chi,\varepsilon} = 1800$–$36\,000$ in the ocean. For comparison, the intermittency factor $\sigma^2_{\ln\$}$ of the superrich (upper 3%) in US personal income, which is close to lognormal, has been measured to be 4.3, giving a Gurvich number $G_\$$ of 600. **Figure 2** shows a lognormality plot of independent deep ocean

samples of $X = C$ averaged over 150 m in the vertical. The axes are stretched so lognormal random variables fit a straight line.

Figure 2 Shows the effects of undersampling errors due to intermittency in attempts to estimate the Cox number C of the stratified layers of the deep ocean, illustrating the 'deep dark mixing paradox.' In 1966 Walter Munk estimated that the vertical turbulent diffusivity of temperature in the deep Pacific Ocean below a kilometer depth should be $K = DC = 1\text{–}2\,\mathrm{cm^2\,s^{-1}}$ with corresponding Cox number of 500–1100. Dropsonde temperature microstructure measurements find $C \approx 30$, more than an order of magnitude less. However, the deep C averages are clearly lognormal, with maximum likelihood estimator C_{mle} values in better agreement with the previous range than with the microstructure range, as shown in **Figure 2**. This matter is still controversial in the oceanographic literature, partly because the tests have either been carried out in shallow high latitude layers where there is no disagreement, or in deep layers where adequate microstructure sampling is impossible. In the shallow main thermocline at 0.3 km, C values are less intermittent and K values are less by a factor of 30 by all methods, including tracer release studies. From the Munk and Gibson value for C, the vertical heat flux is constant at about $6\,\mathrm{W\,m^{-2}}$ at depths in the thermocline between 0.3 and 2 km, consistent with computer models of planetary heat transfer.

Remarkably, the galactic dark matter paradox arises from errors very similar to those leading to the oceanic dark-mixing paradox. Gas emerging from the Big Bang plasma condensed to form a primordial fog of widely separated objects, each with the mass of a small planet. These PFPs entered into nonlinear gravitational accretional cascades to form stars a million times more massive, and their number density n became lognormal with Gurvich numbers G_n near 10^6. Only about 1 in 30 finds its way into a star. The rest are now dark and frozen, thirty million per star in a galaxy, dominating the interstellar and inner-halo galactic dark matter. Star microlensing surveys have failed to detect these objects, and have excluded their existence assuming a uniform pdf rather than the expected intermittent lognormal probability density function for n that explains this questionable interpretation.

Turbulence and Fossil Turbulence Definitions

Turbulence is defined as a rotational, eddy-like state of fluid motion where the inertial-vortex forces of the eddies are larger than any of the other forces which tend to damp the eddies out. The inertial-vortex force $\vec{F}_I = \vec{v} \times \vec{\omega}$ produces turbulence, and appears in the Newtonian momentum conservation equations,

$$\frac{\partial \vec{v}}{\partial t} = -\nabla B + \vec{v} \times \vec{\omega} + \vec{F}_{\mathrm{v}} + \vec{F}_{\mathrm{C}} + \vec{F}_{\mathrm{B}} + \ldots;$$

$$B = \frac{p}{\rho} + \frac{v^2}{2} + gz \qquad [1]$$

where $\vec{v}$ is the velocity field, $\vec{\omega} = \nabla \times \vec{v}$ is the vorticity, B is the Bernoulli group of mechanical energy terms, p is pressure, ρ is density, g is gravity, z is up, $\vec{F}_v = \nu \nabla^2 \vec{v}$ is the viscous force, ν is the kinematic viscosity, $\vec{F}_{\mathrm{C}} = 2\vec{v} \times \vec{\Omega}$ is the Coriolis force, and $\vec{F}_{\mathrm{B}} = N^2 L$ is the buoyancy force when the buoyancy frequency N is averaged over the largest vertical scale L of the turbulence event (other forces are neglected). The growth of turbulence is driven by $\vec{F}_{\mathrm{I}}$ forces at all scales of the turbulent fluid. Irrotational flows (those with $\vec{\omega} = 0$) are nonturbulent by definition, but supply the kinetic energy of turbulence because the turbulent fluid induces a nonturbulent cascade of the irrotational fluid from large to small scales by sucking irrotational fluid into the interstices between the growing turbulence domains. In turbulent flows, viscous and inertial-vortex ($\vec{v} \times \vec{\omega}$) forces are equal at a universal critical Reynolds number $\nu x/\nu \approx 100$ for separation distances $x \approx 10\,L_{\mathrm{K}}$, where L_{K} is the Kolmogorov length scale

$$L_{\mathrm{K}} \equiv \left[\frac{\nu^3}{\varepsilon}\right]^{1/4} \qquad [2]$$

and ε is the viscous dissipation rate per unit mass.

Fossil turbulence is defined as a fluctuation in any hydrophysical field produced by turbulence that persists after the fluid is no longer turbulent at the scale of the fluctuation. Examples of fossil turbulence are jet contrails, skywriting, remnants of cold milk poured rapidly into hot coffee, and patches of ocean temperature microstructure observed with little or no velocity microstructure existing within the patches. The best-known fossil turbulence parameter in the ocean is the mixed-layer depth, which persists long after it was produced and the turbulence has been damped. Buoyancy forces match inertial-vortex forces in a turbulent flow at the Ozmidov scale

$$L_{\mathrm{R}} \equiv \left[\frac{\varepsilon}{N^3}\right]^{1/2} \qquad [3]$$

where the intrinsic frequency N of a stratified fluid is

$$N \equiv \left[\frac{-g\partial\rho}{\rho\partial z} \right]^{1/2} \qquad [4]$$

for the ambient stably stratified fluid affecting the turbulence. Coriolis forces match inertial-vortex forces at the Hopfinger scale

$$L_{\mathrm{H}} \equiv \left[\frac{\varepsilon}{\Omega^3} \right]^{1/4} \qquad [5]$$

where Ω is the angular velocity of the rotating coordinate system.

Taking the curl of eqn [1] for a stratified fluid gives the vorticity conservation equation

$$\frac{\partial\vec{\omega}}{\partial t} + \vec{v}\cdot\nabla\vec{\omega} = \vec{\omega}\cdot\overleftrightarrow{e} + \frac{\nabla\rho\times\nabla p}{\rho^2} + \nu\nabla^2\vec{\omega} \qquad [6]$$

where the vorticity of fluid particles (on the left side) tends to increase from vortex line stretching by the rate of strain tensor $\overleftrightarrow{e}$ (the first term on the right), baroclinic torques on strongly tilted strong density gradient surfaces (the second term), and decreases by viscous diffusion (the third term). From eqn [6] we see that turbulence events in stably stratified natural fluids are most likely to occur where density gradients are large and tilted for long time periods; for example on fronts, because this is where most of the vorticity is produced.

Formation and Detection of Stratified Fossil Turbulence

Figure 3 shows how turbulence bursts and fossil turbulence patches may form in the interior of the stratified ocean by vorticity forming on a tilted density surface, starting from a state of rest. The longer the density surface is tilted the more kinetic energy is stored in the resulting boundary layers. The boundary layers formed on both sides of the tilted surface become turbulent when the critical Reynolds number is reached. This occurs when the boundary layer thickness is 5–10 L_{K} based on the viscous dissipation rate of the laminar boundary layer (**Figure 3C**). The turbulence sharpens the density gradient, keeping the local Froude number $F(z) = u(z)/zN(z)$ less than $Fr_{\mathrm{crit}} \approx 2$ so that the kinetic energy is stored. Billows form when $Fr(z) \geq 2$ (**Figure 3D**), and the turbulent burst occurs, absorbing all the kinetic energy stored on the tilted density layer. Fossilization begins when buoyancy forces match the inertial vortex forces of the turbulence, at a vertical size of about $0.6\,L_{\mathrm{R}}$ (**Figure 3E**) with viscous dissipation rate ε_{o}. The dissipation rate ε decreases with time during the process so L_{R} decreases as the vertical patch size $L_{\mathrm{P}} \approx L_{\mathrm{Tmax}}$ increases. The fossil turbulence patch does not collapse, even though the interior turbulent motions decrease in their vertical extent. The patch size L_{P} preserves information about the Ozmidov scale L_{Ro} at the beginning of fossilization when the viscous dissipation rate ε is ε_{o}. Thus, from eqn [3] and $L_{\mathrm{Ro}} = 0.6\,L_{\mathrm{R}}$ we have the expression

$$\varepsilon_{\mathrm{o}} = 0.4 L_{\mathrm{P}}^2 N^3 \qquad [7]$$

from which we can estimate ε_{o} from measurements of $L_{\mathrm{P}} \approx L_{\mathrm{Tmax}}$ and N long after the turbulence event. Because the saturated internal waves of fossil vorticity turbulence have frequency N, they propagate vertically, and produce secondary turbulence events above and below the fossil turbulence patch (**Figure 3F**). Secondary turbulent events also form at the top and bottom of the fossil because these strong gradient surfaces are also likely to be tilted.

Motions of the ocean are inhibited in the vertical direction by gravitational forces, so that the turbulence and fossil vorticity turbulence kinetic energy is mostly in the horizontal direction. In eqn [5], Ω is the vertical component of the Earth's angular velocity and approaches zero at the equator since $\Omega = \Omega_{\mathrm{o}}\sin\theta$, where θ is the latitude. Large-scale winds and currents develop at equatorial latitudes because they are unchecked by Coriolis forces. These break up into horizontal turbulence which can also cascade to large scales before fossilization by Coriolis forces at L_{H} scales. Ozmidov scales L_{R} and Hopfinger scales L_{H} for the dominant turbulent events of particular layers, times, and regions of the ocean cover a wide range, with typical maximum values $L_{\mathrm{R}} = 3$–$30\,\mathrm{m}$ and $L_{\mathrm{H}} = 30$–$500\,\mathrm{km}$ occurring where ε is large.

Quantitative Methods

A patch of temperature, salinity, or density microstructure is classified according to its hydrodynamic state by means of hydrodynamic phase diagrams as shown in **Figure 1** (insert), which compare parameters of the patch to critical values. For the patch to be fully turbulent, both the Froude number $\mathrm{Fr} = U/NL$ and the Reynolds number $\mathrm{Re} = UL/\nu$ must be larger that critical values from our definition of turbulence. If both are subcritical the patch is classified as completely fossilized. Most oceanic microstructure patches are found in an intermediate

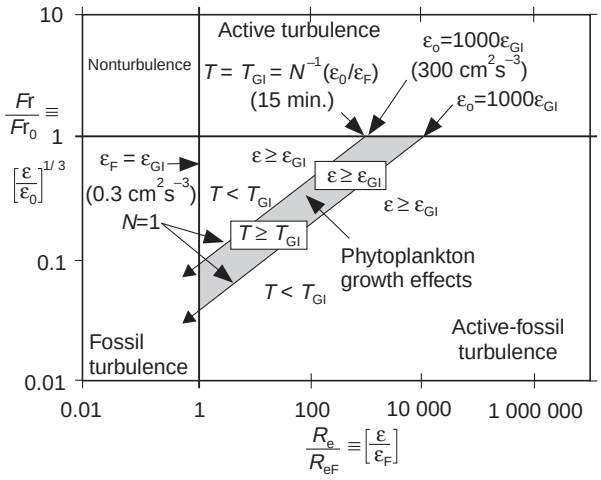

Figure 4 Hydrodynamic phase diagram showing the domain of phytoplankton growth effects corresponding to measured values of $\varepsilon_{GI} = 0.3\,\mathrm{cm^2\,s^{-3}}$ and $T_{GI} = 15\,\mathrm{min}$ (From Gibson and Thomas 1995 JGR 100, 24 841) for growth inhibition (GI) of a red tide dinoflagellate.

state, termed partially fossilized, where *Fr* is subcritical and *Re* is supercritical. This means that the largest turbulent eddies have been converted into saturated internal waves, but smaller-scale eddies exist that are still overturning and fully turbulent. A variety of hydrodynamic phase diagrams have been constructed as fossil turbulence theory has evolved, but all have active, active-fossil, and completely fossil quadrants. **Figure 4** shows a hydrodynamic phase diagram applied to turbulence-fossil–turbulence-phytoplankton growth interaction.

Growth rates of various phytoplankon species are extremely sensitive to both turbulence and the duration of the turbulence. Laboratory experiments reveal that red tide dinoflagellates have two thresholds for growth inhibition; dissipation rate $\varepsilon \geq \varepsilon_{GI}$ for turbulence, and $T \geq T_{GI}$ for the duration T of turbulence with $\varepsilon \geq \varepsilon_{GI}$ (apparently to detect oceanic fossil turbulence from its greater persistence). If the dissipation rate ε exceeds about $\varepsilon_{GI} = 0.3\,\mathrm{cm^2\,s^{-3}}$ for periods T more than $T_{GI} = 15\,\mathrm{min}$ a day for such microscopic swimmers they stop reproducing and the population dies in a few days. Shorter-duration turbulence events are ignored, no matter how powerful. Diatom growth in the laboratory and field reacts positively to turbulence events with more than several minutes persistence. The hypothesis matching this behavior is that both classes of species have evolved methods of hydrodynamic pattern recognition so that they can maximize their chances of survival with respect to their swimming abilities.

Dinoflagellate red tides occur when nutrient-rich upper layers of the sea experience several days of sun with weak winds and waves so that they become strongly stratified. The diatoms settle out of the light zone so that the dinoflagellates can bloom. However, when waves appear with sufficient strength to break and mix the surface layer, this may be detected by the phytoplankton from the long persistence time $T > T_{GI}$ of the fossil-vorticity-turbulence patches produced by breaking waves. It is supposed that when such fossil-vorticity-turbulence patches are detected, both phytoplankton species adjust their growth rates in anticipation of an upcoming sea-state change from strongly stratified to well mixed in order to maximize their survival rates according to their swimming abilities. The expression derived by the author for the persistence time of $\varepsilon \geq \varepsilon_F$ in a fossil turbulence patch before it becomes completely fossilized is $T = N^{-1}\varepsilon_o/\varepsilon_F$, where the Reynolds number ratio $Re_o/Re_F = \varepsilon_o/\varepsilon_F = \varepsilon_o/30\nu N^2$ (top of **Figure 4**). The shaded gray zone of the hydrodynamic phase diagram in **Figure 4** shows estimates of N and ε_o that would inhibit growth of a particular red tide dinoflagellate species with ε_{GI} and T_{GI} values known from laboratory measurements.

See also

Dispersion and Diffusion in the Deep Ocean. Phytoplankton Blooms.

Further Reading

http://xxx.lanl.gov http://www-acs.uscd.edu/ ~ ir118.

Gibson CH (1991) Kolmogorov similarity hypotheses for scalar fields: sampling intermittent turbulent mixing in the ocean and galaxy. In: *Turbulence and Stochastic Processes: Kolmogorov's Ideas 50 Years On*, Proceedings of the Royal Society London, Ser. A, V 434 (N 1890) 149–164.

Gibson CH (1996) Turbulence in the ocean, atmosphere, galaxy, and universe. *Applied Mechanics Reviews* 49 (5) 299–315.

Gibson CH (1999) Fossil turbulence revisited. *Journal of Marine Systems* 21: 147–167.

Thomas WH, Tynan CT and Gibson CH (1997) Turbulence–phytoplankton interrelationships. In: *Progress in Phycological Research* Ch. 5, Vol. 12, Chapman DJ and Round FE (eds) Biopress Ltd.